

Article

# Optimization Research on Aluminum-Nickel Alloy Milling Using the Taguchi Method

Shang-Ping Wei<sup>1</sup>, Ah-Der Lin<sup>2</sup>, Chun-Wel Chang<sup>1</sup>, Yun-Chen Chien<sup>1</sup>, Yo-Tsai Tsai<sup>1</sup>  
and Chao-Ming Hsu<sup>1,\*</sup>

<sup>1</sup> Department of Mechanical Engineering, National Kaohsiung University of Science and Technology; Kaohsiung City 80778, Taiwan; sm10916@yahoo.com.tw (S.-P. W.), F111142168@nkust.edu.tw (C.-W. C.), F112142119@nkust.edu.tw (Y.-C. C.)

<sup>2</sup> Department of Mechanical Engineering, Cheng Shiu University, Kaohsiung City 83347, Taiwan; 0549@gcloud.csu.edu.tw  
\* Correspondence: jammy@nkust.edu.tw

**Received:** Dec 22, 2024; **Revised:** Jan 14, 2025; **Accepted:** Feb 13, 2025; **Published:** Mar 30, 2025

**Abstract:** The study aimed to explore the machining parameters of general milling and used the Taguchi method to obtain the optimal parameter combination and contribution value of surface roughness. Essential process parameters were identified, including spindle speed, feed rate, depth of cut, and tool diameter. Then, in the experiment, the spindle speed parameters were set to 2000rpm, 2500rpm, and 3000rpm. The feed speed parameters were set to 400mm/min, 500mm/min, and 600mm/min. The milling depth parameters were set to 0.2mm, 0.4mm, and 0.6mm. Based on the experimental results, the following conclusions were drawn. The optimization factors for surface roughness in general milling were spindle speed A2 (2500rpm), feed speed B2 (500mm/min), cutting depth C2 (0.4mm), and tool diameter D3 (4mm). After individual quality optimization analysis and verification experiments, the optimized surface roughness measurement value was Ra 0.23 $\mu$ m, which was an increase of 56.52% compared to the average best value of Ra 0.36 $\mu$ m in 9 sets of tests.

**Keywords:** Taguchi method, Silicon carbide, Conventional grinding, Surface roughness, Residual stress

## 1. Introduction

Milling is one of the most commonly used machining processes, and precision is the most challenging aspect. High-speed CNC milling technology has been dramatically developed in mold manufacturing. Generally speaking, machining accuracy depends on controllable factors. Due to the significant demand in the mold industry, high-speed CNC milling technology has met the processing conditions of the mold industry. High-speed machines improved manufacturing efficiency, work surface finish, and precise dimensional accuracy [1]. CNC vertical end mills have gained wide acceptance in modern enterprises due to their fast material removal rates and ability to produce complex surfaces with extremely high precision. The innovative end-milling process was used in the industry for metal removal due to faster material rates, resulting in a good surface finish. The best applications were in the automotive and aerospace sectors, where slots, molds, and dies were manufactured [2].

In recent years, the aviation industry has developed rapidly, and the selection of materials has increasingly focused on conditions such as high hardness, high-temperature resistance, and corrosion resistance. Although various advanced materials were gradually being widely used, their properties were mostly high hardness or brittle materials, making them difficult to process with traditional processing techniques. It was extremely easy to cause tool loss and workpiece fragmentation during machining. Therefore, it was still necessary to find the optimal processing parameters and combinations [3–5].

## 2. The Basic Theory of Experiment

### 2.1 Theoretical Basis of Milling Processing Technology

Milling was a vital processing technology in traditional manufacturing technology. The processing method was mainly through the high-speed rotation of end mills or face mills for cutting, often applied to the material surface or internal feature contours. Milling operations were characterized by good surface quality and dimensional accuracy. Milling process of a wide range of materials, such as metals, carbides, carbide metals, ceramics, glass, and composite brittle materials.

### 2.1.1 Grinding Force

In the metal cutting process, cutting force was a key factor affecting tool-workpiece vibration and workpiece dimensional accuracy. Establishing an accurate and reliable cutting force model by analyzing cutting forces was the basis for chatter prediction and an essential prerequisite for optimizing cutting parameters. The accuracy of cutting force prediction largely depended on the cutting force coefficient of the material, and the identification of the cutting force coefficient was the core of the cutting force model. Therefore, the cutting force coefficient was the main parameter in the cutting force model, and its accurate identification has an essential impact on the cutting process research.

The cutting force was the shear force generated by shearing in the shear zone, and the blade force was generated by friction on the flank surface of the cutting edge. The shear force was expressed as the product of the tangential force coefficient  $K_{tc}$ , the error force coefficient  $K_{rc}$ , the torsional force coefficient  $K_{ac}$ , and the loss force. The blade force was expressed as the product of the tangential blade force coefficient  $K_{te}$ , the die blade force coefficient  $K_{re}$ , the die blade force coefficient  $K_{ae}$ , and the cutting width.  $K_{tc}$ ,  $K_{rc}$ ,  $K_{ac}$ ,  $K_{te}$ ,  $K_{re}$ , and  $K_{ae}$  were collectively called cutting coefficients.

$$\begin{aligned}
 dF_t &= K_{tc}a_c d(a_p) + K_{te}d(l) \\
 dF_r &= K_{rc}a_c d(a_p) + K_{re}d(l) \\
 dF_a &= K_{ac}a_c d(a_p) + K_{ae}d(l)
 \end{aligned}
 \tag{1}$$

The basic formula of the instantaneous rigid force model was (1), where  $dF_t$ ,  $dF_r$ , and  $dF_a$  were the tangential, radial, and axial cutting force elements, respectively.  $d(l)$ ,  $d(a_p)$ , and  $a_c$  were the cutting edge length, axial cutting depth, and cutting thickness, respectively.  $K_{tc}$ ,  $K_{rc}$ , and  $K_{ac}$  were the tangential, radial, and axial cutting force coefficients.  $K_{te}$ ,  $K_{re}$ , and  $K_{ae}$  are the tangential, radial, and axial blade force coefficients. The above six cutting force coefficients were considered constants in the average cutting force model. Its specific value was obtained through cutting force coefficient identification experiments [4].

### 2.1.2 Material Removal Rate (MRR)

MRR material removal rate, which represented the area of material removed within a time, was a standard for measuring manufacturing efficiency and an essential parameter in the processing process. The higher the MRR, the more efficient the operation and generally shortens the cycle time. The basic schematic and terminology used for calculating the response material removal rate [6,7].

- N = tool speed
- n = number of teeth on the tool
- W = cutting width
- T = Tool depth
- V = cutting speed
- L = pass or cutting length
- $f_m$  = table (machine tool) feed
- $f_t$  = tool feed/number of teeth
- D = tool diameter
- Table feed:  $f_m = f_t \times N \times n$
- Cutting time:  $CT = L/f_m$

The metal removal rate for end milling is calculated as follows:

$$MRR = \frac{\text{Volume Re moved}}{\text{Cutting Time}} = \frac{L \times W \times t}{CT} = W \times t \times f_m$$

## 2.2 Taguchi-style Quality Engineering

Taguchi quality engineering was a robust design method proposed by Japanese quality expert Dr. Genichi Taguchi. It was generally called the Taguchi Method or Taguchi Methods of Robust Design. Taguchi defined product quality as the loss a product brings to society from when it was shipped to the customer. Some of these losses were caused by the deviation of the product's functional characteristics from its expected target value, which were called functional variation losses. Uncontrollable factors that caused product functional characteristics to deviate from target values were called noise factors and divided into external factors, manufacturing defects, and product deterioration. Control factors were the most essential part of the experimental design. As many factors as possible were used to identify non-significant variables as early as possible. Taguchi used signal-to-noise ratio (S/N) as a quality characteristic for selection. The signal-to-noise ratio instead of standard deviation was used as the measurable value because as the mean decreased, the standard deviation decreased and vice versa. There was no minimized standard deviation first and then the mean to the target. Taguchi found empirically that a two-stage optimization procedure involving a signal-to-noise ratio did give a combination of parameter levels. Where the standard deviation was minimized while keeping the mean on target [8–13]. This means that the engineered system behaves in such a way that the manipulated factors of production are divided into three categories:

1. Control factors that affect process variability measured by signal-to-noise ratio.
2. Signal factors do not affect signal-to-noise ratio or process average.
3. Factors that do not affect the signal-to-noise ratio or process mean.

Two applications where the signal-to-noise ratio concept was useful were improving quality and measurements by reducing variability. When the characteristics persist, the signal-to-noise ratio characteristics fall into three categories:

- (1). nominal is the best characteristic:  $S/N=10\log\sigma_y^2$
- (2). smaller the better characteristics:  $S/N=-10\log\ln^2\sigma_y^2$
- (3). larger the better characteristics:  $S/N=-10\log\ln^2\sigma_y^2$

For each feature type, through the above signal-to-noise ratio transformation, the higher the signal-to-noise ratio, the better the result [14].

## 3. Materials and Methods

### 3.1 Experimental Materials & Tools

#### 3.1.1. Titanium Silicon Tungsten Steel Knife

The cutting tool diameters required for this experiment were 2mm, 3mm, and 4mm tungsten steel end mills. The coating was titanium silicon, and the HRC hardness was 50, as shown in Figure 1(a).

#### 3.1.2. Aluminum-Nickel Alloy

The material of this experiment was aluminum-nickel alloy, which has corrosion resistance and high-temperature stability. It was a square material with a size of 290\*59\*15mm, as shown in Fig. 1(b).



**Fig. 1.** Experimental materials and cutting tools (a) Al-nickel alloy (b) Titanium silicon tungsten steel knife.

### 3.2 Experimental Equipment

This experimental machine was a CNC three-axis milling machine, S-Plus 10, manufactured by Xiehong Industrial Co., Ltd. Its processing mode was to hold the tool with the tool arbor. It was processed using the cutting method of a rotating tool. Use a vise

to fix the workpiece. The three axes of X, Y, and Z controlled the plane movement of the machine table, which was positioned by the vise, to complete the processing. The appearance of the machine as shown in Fig.2(a).

The surface roughness measuring instrument was the SJ-410 surface roughness measuring machine produced by Mitutoyo. The detection method was differential inductance. By pressing the probe to the surface of the measurement object, adjusting it to the appropriate measurement depth, and moving the driving part (X-axis) to measure the surface roughness, as shown in Fig. 2(b).



**Fig. 2.** Experimental equipment (a) CNC processing machine S-Plus 10 (b) Surface roughness measuring instrument SJ-410.

### 3.3 Experimental Methods and Procedures

#### 3.3.1 Overview

This article aimed to use general milling machining methods for unique materials. According to the literature review, it is currently known that some scholars have used existing alloys in aerospace and the Taguchi method to design processing parameters for milling. However, the main experimental processing parameters were micro-milling for experimental design, which was not used to achieve the required work efficiency in modern factories. The study used the Taguchi method with general milling and cutting to verify the practicability of the processing method. Then, the processing parameter set with optimal mechanical properties was analyzed according to the Taguchi method, and its optimal parameters were verified.

#### 3.3.2 Research on Experimental Parameter Level Setting

After selecting the key processing control factors, the next step was to set the experimental parameter levels. The primary purpose of this experiment was to determine the optimal processing parameters for surface roughness using the Taguchi method. To ensure the reliability of the selected parameters, a one-factor-at-a-time approach was adopted, referring to relevant literature and selecting parameters suitable for this experiment as the parameter level design of the Taguchi method experiment.

According to the literature [10,11], feed speed was the most critical factor affecting surface roughness during milling. Followed by ultrasonic power, cutting speed, and cutting depth. Therefore, this experiment selected spindle speed, feed speed, cutting depth, and tool diameter as processing control factors.

##### (1) Spindle speed parameters

This experiment's spindle speed parameter settings were based on a review of multiple related studies, with special reference to the "Experimental Design of Aluminum Alloy Milling Processing in the Aviation Industry" published by Andrei Victor Sandu et al. in 2019 [9]. The spindle speed in this study ranged from 495 rpm to 600 rpm but was adjusted to match the experimental site conditions. Therefore, the spindle speed levels for this experiment were set at 2000 rpm, 2500 rpm, and 3000 rpm.

##### (2) Feed speed parameters

The feed speed parameters also referred to the relevant literature on spindle speed. Its range was 495 mm/min to 660 mm/min. However, this range was mainly used for special alloys, and the effect of the Taguchi method experiments might need to be revised. Therefore, the parameters were adjusted to 400 mm/min, 500 mm/min, and 600 mm/min.

##### (3) Cutting depth parameter

The planning cutting depth parameters were reviewed in the literature. Finally, we referred to the research published by Andrei Victor Sandu et al. in 2020 [8]. The parameter range of this study was 0.04 mm to 0.14 mm. Still, considering the experimental

equipment and material characteristics, it was observed that equipment accuracy and material differences need to be adjusted. Therefore, the cutting depth parameters were set to 0.2 mm, 0.4 mm, and 0.6 mm.

(4) Tool diameter planning

There were few related studies on this control factor, but the "Research on Cutting Forces in Ultrasonic Vibration-Assisted Milling Processing" published by Girish Chandra Verma, Pulak Mohan Pandey, et al. in 2019 [15] pointed out that the selection of tool diameter affects the surface roughness value. Since this experiment was for general milling processing, the Ø3 mm titanium silicon tungsten steel tool was selected as the essential experimental tool, and Ø2 mm, Ø3 mm, and Ø4 mm were used as experimental parameters for testing.

3.3.3 Create L9(3<sup>4</sup>) Orthogonal Table

There were four factors in this experiment, each with its own three levels, and interactions were not considered in this experiment. Based on the calculation of the degrees of freedom of the factors and the degrees of freedom of the orthogonal table, it was judged to use three levels of orthogonal tables. Finally, the L9 orthogonal table was selected for this experiment. This experiment focused on the discussion of surface roughness characteristics. The smaller the value, the better if the surface roughness could be more exceptional. Therefore, in this study, the surface roughness adopted a slight characteristic.

**Table 1.** Control factors and parameter level planning table.

| Control Factors |                     | Parameter Levels |         |         |
|-----------------|---------------------|------------------|---------|---------|
|                 |                     | Level 1          | Level 2 | Level 3 |
| A               | Spindle Speed (rpm) | 2000             | 2500    | 3000    |
| B               | Feed Rate (mm/min)  | 400              | 500     | 600     |
| C               | Depth of Cut (mm)   | 0.2              | 0.4     | 0.6     |
| D               | Tool Diameter (mm)  | 2                | 3       | 4       |

3.3.4 Experimental Processing

This experimental processing was repeated four times for each set of parameter-level combinations to obtain experimental accuracy. According to the processing position, from top to bottom and left to right, y1, y2, y3, y4, and y5 were the processing numbers. The experimental processing range of its nine groups was designed to be 32 mm long, 58.8 mm wide, and 3 mm apart. To accurately locate the y1 processing position, set the y1 processing range of 12 mm, leaving 3mm above and 3mm on the left for y1 position identification. The experimental processing positions and position numbers as shown in Fig.3.

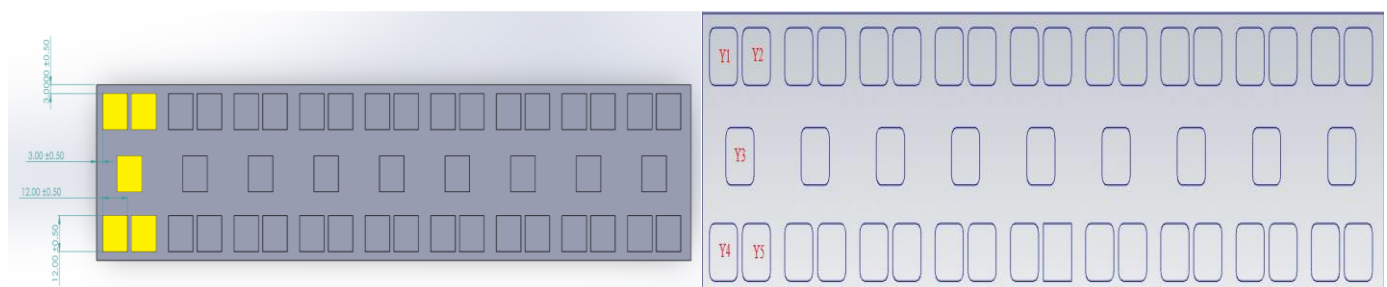


**Fig. 3.** Experimental processing position.

3.3.5 Model Establishment - Material Boundary and Processing Tool Settings

After completing the establishment of the L9 orthogonal table and experimental processing planning, to carry out experimental processing smoothly, the model must be established first and then moved into the internal storage system of the numerical control processing machine.

First, the material boundaries and processing tool settings must be set before establishing the experimental processing model. The material boundary and tool settings were set according to the specifications of the experimental material and end mill. The experimental material specifications were a 280\*58.8\*15mm cuboid, and the origin position was set at the lower left corner above the part. The end mill specifications were 60mm in total length, 6.0mm in shank diameter, 2 mm~4 mm in tool diameter, and 6 mm~12 mm in tool length.

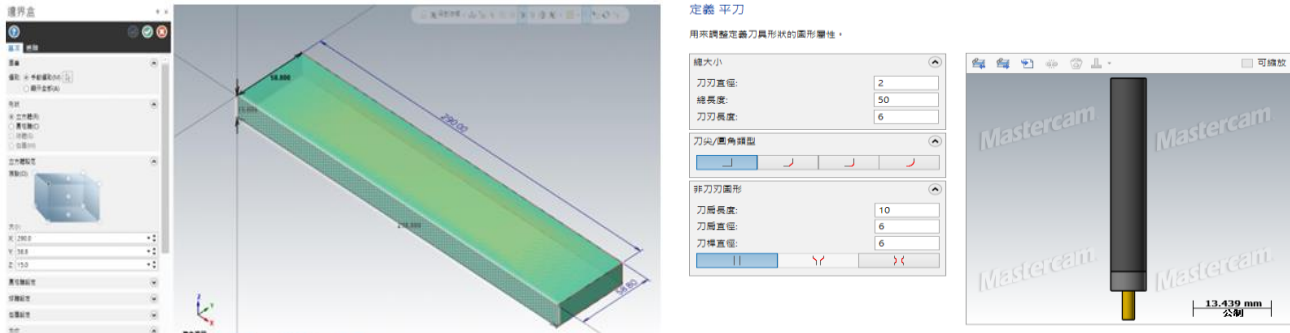


Fig. 4. Model establishment.

After completing the material boundary and processing tool settings, the material manufacturing method, this time, was casting. The finished product has surface unevenness and poor parallelism, which required establishing a processing model for processing. After the problem of material unevenness was solved, this experimental processing was carried out. The surface and parallelism processing model parameters were set according to the parameter level: spindle speed 4000 rpm, feed speed 60 mm/min, and step amount 0.15mm. The processing depth was set to 0.5mm and processed in five steps of 0.1mm each time. The tool path setting for surface milling as shown in Fig.5.

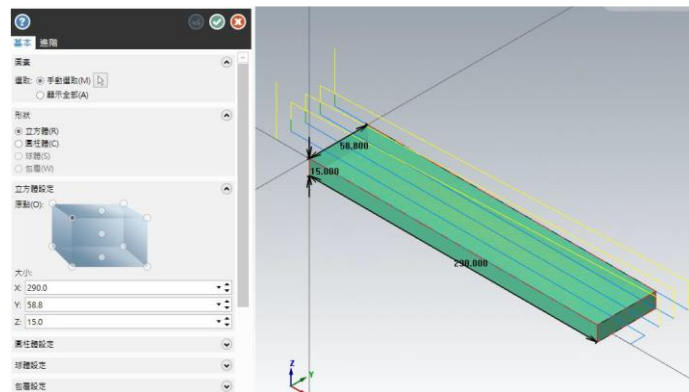


Fig. 5. Tool path simulation diagram of surface milling.

### 3.3.6. Experimental Parameter Processing

After the material surface was milled, the next step was to bring the parameter levels and experimental processing planning table designed by Taguchi's orthogonal table into actual processing. This experiment explored the general milling processing methods. Each processing method has nine sets of experiments, totaling 18 sets of experiments. The tool path for experimental machining.

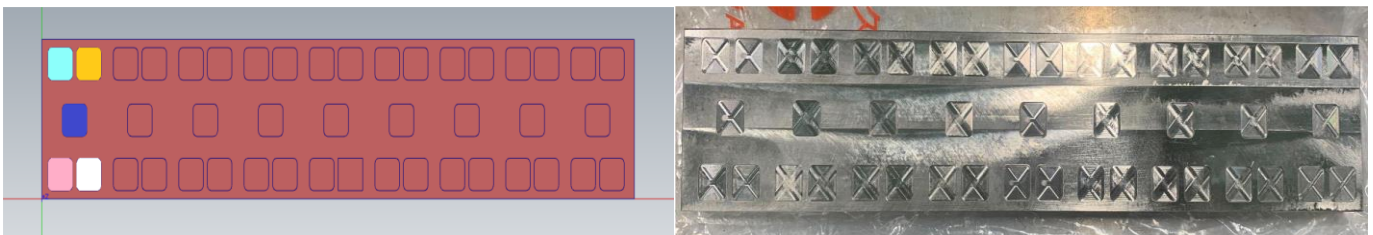


Fig. 6. Experimental processing path simulation and finished product.

### 3.3.7. Measurement of Experimental Finished Products

The surface roughness measurement of this experimental processing was carried out using a surface roughness measuring instrument. The measurement method as shown in Figure 3-11. Nine positions were expected to be selected as measurement points at each processing position, and the average of 12 measurement values was used as a Taguchi measurement result. There was a total of 48 measurement points at four processing positions. A schematic diagram of the measurement points was shown. The measurement parameters of the surface roughness measuring instrument were set as follows: standard ISO1997, measurement moving speed 0.5mm/s, reference length (ln) 0.08mm, and measurement length set to 0.24mm. The measurement parameter settings as shown in Fig.7.

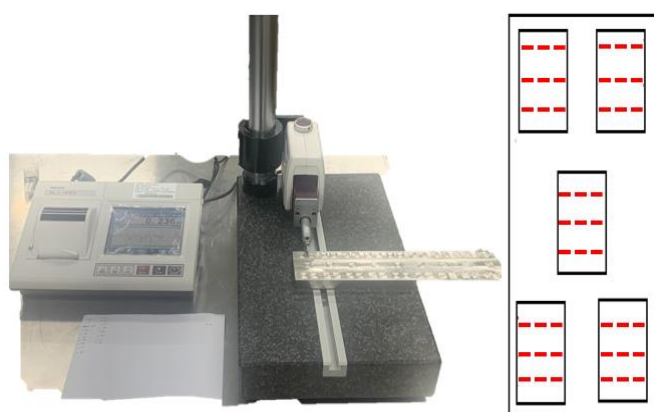


Fig. 7. Schematic diagram of measurement methods and measurement points.

## 4. Results and Discussion

### 4.1 General Milling Analysis and Measurement Results

#### 4.1.1 Surface Roughness Measurement and Analysis Results

Milling results for surface roughness analysis. The best surface roughness value was Ra 0.225 (um) in the eighth group, while the worst was Ra 0.447 (um) in the ninth group. The highest values of surface roughness measurement occur on both sides of the path edge. It was speculated that the milling cutter tool diameter was small, the cutting amount was large, and the tool wear caused incomplete processing. Table 2 and Fig.8 show the surface roughness measurement results of each group of experiments.

Table 2. General milling surface roughness Ra measurement results.

| Number          | y1<br>Measured Value (um) | y2<br>Measured Value (um) | y3<br>Measured Value (um) | y4<br>Measured Value (um) | y5<br>Measured Value (um) | Average (um) | Standard Deviation |
|-----------------|---------------------------|---------------------------|---------------------------|---------------------------|---------------------------|--------------|--------------------|
| 1               | 0.320                     | 0.317                     | 0.357                     | 0.447                     | 0.472                     | 0.383        | 0.072              |
| 2               | 0.312                     | 0.308                     | 0.289                     | 0.311                     | 0.335                     | 0.311        | 0.016              |
| 3               | 0.398                     | 0.398                     | 0.438                     | 0.430                     | 0.334                     | 0.400        | 0.041              |
| 4               | 0.292                     | 0.203                     | 0.224                     | 0.197                     | 0.244                     | 0.232        | 0.038              |
| 5               | 0.384                     | 0.250                     | 0.510                     | 0.469                     | 0.440                     | 0.410        | 0.101              |
| 6               | 0.436                     | 0.374                     | 0.410                     | 0.408                     | 0.377                     | 0.401        | 0.026              |
| 7               | 0.492                     | 0.470                     | 0.403                     | 0.387                     | 0.405                     | 0.431        | 0.046              |
| 8               | 0.276                     | 0.246                     | 0.229                     | 0.179                     | 0.195                     | 0.225        | 0.039              |
| 9               | 0.469                     | 0.453                     | 0.397                     | 0.476                     | 0.439                     | 0.447        | 0.031              |
| Overall Average |                           |                           |                           |                           |                           | 0.36         | 0.046              |

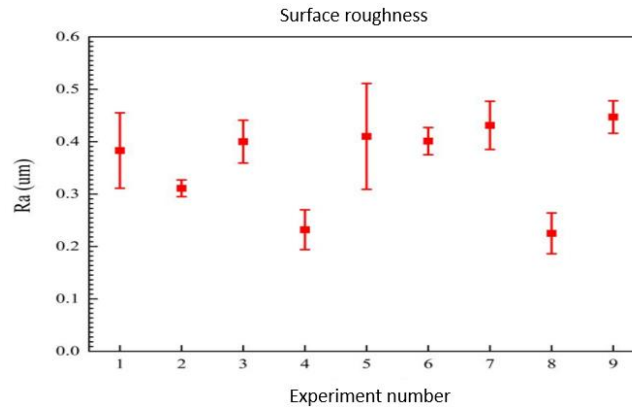


**Fig. 8.** Conventional milling surface roughness.

#### 4.2 Milling Single Quality Optimization Analysis Results

##### 4.2.1 Single Quality Optimization Analysis Results of Surface Roughness

This article calculated the S/N ratio based on the surface roughness measurement results of the L9 orthogonal table. The calculation results as shown in Table 3. The response table and response diagram of each control factor were calculated and controlled using the S/N ratio of the small characteristic formula. The calculation results were as follows. The significance of the control factors was judged through the control factor response chart in order of feed speed, spindle speed, milling depth, and tool diameter. There was selected the best combination from the response table as A2 B2 C2 D3, that was, spindle speed 2500 (rpm), feed speed 500 (mm/min), milling depth 0.15 (mm), and tool diameter 4 (mm).

**Table 3.** Surface roughness data and S/N ratio.

| A                   | B                  | C                 | D                  | Surface Roughness (um) | S/N Ratio (dB) |
|---------------------|--------------------|-------------------|--------------------|------------------------|----------------|
| Spindle Speed (rpm) | Feed Rate (mm/min) | Depth of Cut (um) | Tool Diameter (mm) |                        |                |
| 1                   | 1                  | 1                 | 1                  | 0.383                  | 8.219          |
| 1                   | 2                  | 2                 | 2                  | 0.311                  | 10.128         |
| 1                   | 3                  | 3                 | 3                  | 0.400                  | 7.930          |
| 2                   | 1                  | 2                 | 3                  | 0.232                  | 12.594         |
| 2                   | 2                  | 3                 | 1                  | 0.410                  | 7.531          |
| 2                   | 3                  | 1                 | 2                  | 0.401                  | 7.918          |
| 3                   | 1                  | 3                 | 2                  | 0.431                  | 7.262          |
| 3                   | 2                  | 1                 | 3                  | 0.225                  | 12.850         |
| 3                   | 3                  | 2                 | 1                  | 0.447                  | 6.977          |

Average = 9.046 (dB)

**Table 4.** Response table of each control factor level.

| Parameter levels | Control factors     |                    |                   |                    |
|------------------|---------------------|--------------------|-------------------|--------------------|
|                  | A                   | B                  | C                 | D                  |
|                  | Spindle Speed (rpm) | Feed Rate (mm/min) | Depth of Cut (um) | Tool Diameter (mm) |
| 1                | 8.759               | 9.358              | 9.662             | 7.576              |
| 2                | 9.348               | 10.170             | 9.900             | 8.436              |
| 3                | 9.030               | 9.043              | 7.575             | 11.125             |
| \Delta           | 1.665               | 9.043              | 1.061             | 1.160              |
| Ranking          | 4                   | 2                  | 3                 | 1                  |

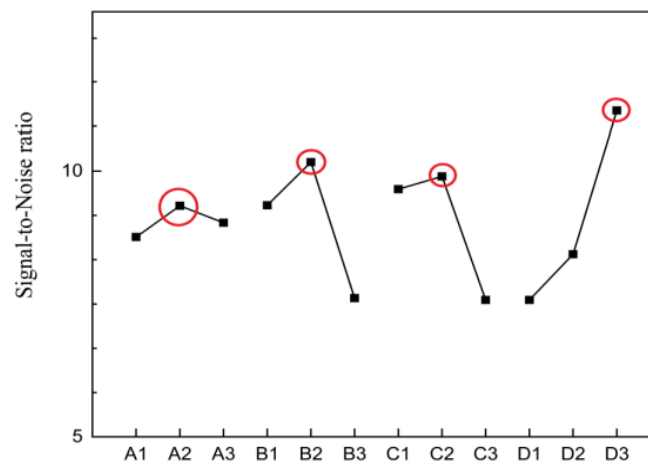


**Fig. 9.** Response chart of each control factor level.

### 4.3 Taguchi Optimal Prediction

#### 4.3.1 Optimal Prediction of Surface Roughness

S/N ratio of optimized predicted value of surface roughness. The S/N ratio calculation formula 4-1 of the optimized predicted value is as follows:

$$\mu_{A2B2C2D3} = \bar{T} + (A2 - \bar{T}) + (B2 - \bar{T}) + (C2 - \bar{T}) + (D3 - \bar{T}) = A2 + B2 + C2 + D3 - 3\bar{T} \quad (2)$$

In Formula (2), T is the overall average S/N ratio. Put the value into Formula (2) to get the S/N ratio of the following optimized predicted values.

$$\mu_{A2B2C2D3} = 9.348 + 10.170 + 9.900 + 11.125 - 3(9.046) = 11.125(\text{dB}) \quad (3)$$

Based on the above results, it can be seen that the predicted S/N ratio of the optimized experiment was more significant than any experimental combination of the S/N ratio of the nine groups of experiments in the L9 orthogonal table. This means the optimized parameter design has an improvement effect, but verification experiments were still needed to confirm its accuracy.

### 4.4 General Milling Parameter Optimization Verification

General milling parameter optimization verification The best parameter combination selected from the reaction table was A2 B2 C2 D3. The parameter levels were spindle speed 2500rpm, feed speed 500mm/min, cutting depth 0.4mm, and tool diameter ø4mm. A verification experiment was conducted using the optimized parameter levels to verify whether the combination was optimal, and a total of five groups were tested. The verification results showed that the surface roughness Ra was 0.23µm, and the signal-to-noise ratio was 12.687dB, as shown in Table 5. The error value between the experimental signal-to-noise ratio and the

predicted value of 11.125 dB was 12.312%, as shown in Table 6. The comparison results showed that the optimized parameter combination has higher accuracy. Figure 8 shows the verification of the optimized surface roughness parameters.

**Table 5.** Response table of each control factor level.

| A                   | B                  | C                 | D                  | Surface Roughness Ra(um) | S/N Ratio (dB) |
|---------------------|--------------------|-------------------|--------------------|--------------------------|----------------|
| Spindle Speed (rpm) | Feed Rate (mm/min) | Depth of Cut (um) | Tool Diameter (mm) |                          |                |
| 2500                | 500                | 0.4               | 4                  | 0.23                     | 12.687         |

**Table 6.** Responses to each control factor level.

| S/N ratio of predicted value | S/N ratio of the experiment | Surface Roughness Ra(um) | Error value (%) |
|------------------------------|-----------------------------|--------------------------|-----------------|
| 11.125                       | 12.687                      | 0.23                     | 12.312          |

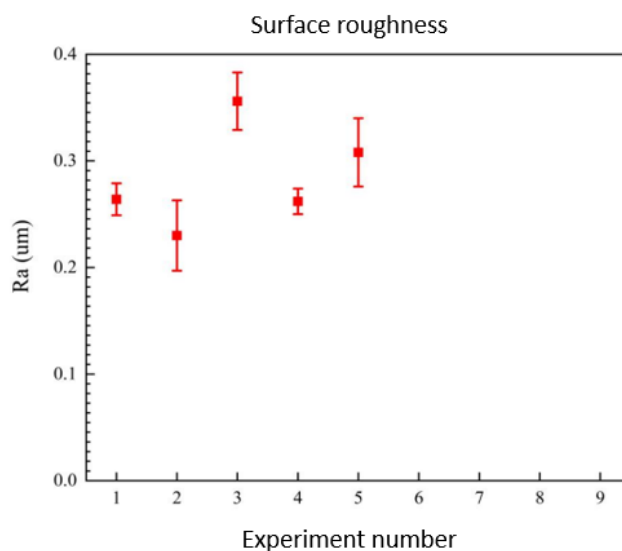


**Fig. 10.** Experimental measurement results of surface roughness optimization parameters.

#### 4. Conclusion

The study used standard milling tools to analyze the surface roughness of aluminum-nickel alloy workpieces. The orthogonal table of the Taguchi method was used to design the experimental parameter combination to obtain the optimal single-quality parameter combination. Analysis was then performed to determine the optimal parameter combination, and the experimental results were analyzed and discussed. The conclusions were as follows: 1. For the surface roughness of ordinary milling, the optimization factors are spindle speed A2 (2500 rpm), feed B2 (500 mm/min), cutting depth C2 (0.4mm), and tool diameter D. After single-quality optimization verification experiments, the optimized ordinary milling surface roughness measurement result was Ra 0.23 μm, which was 56.52% higher than the average optimal value.

**Author Contributions:** All authors contributed equally to this work.

**Funding:** This article results from Project 113TUE25-2 funded by the Ministry of Education.

**Acknowledgments:** The author is writing to express sincere gratitude to the Ministry of Education for its support in enabling the smooth implementation of this project.

**Conflicts of Interest:** The authors declare no conflict of interest.

## References

1. Kar, B.C.; Panda, A.; Kumar, R.; Sahoo, A.K. Research trends in high speed milling of metal alloys: A short review. *Mater. Today Proc.* **2020**, *26*, 2657–2662. <https://doi.org/10.1016/j.matpr.2020.02.564>
2. Raikar, N.A.; Ramashiva, R.; Yathish, N. et al. Ultrasonic Machining Process. *J. Mech. Eng. Res.* **2019**, *3*(11), 82–89.
3. Sun, J.; Guo, Y.B. A comprehensive experimental study on surface integrity by end milling Ti–6Al–4V. *J. Mater. Process. Technol.* **2009**, *209*, 4036–4042. <https://doi.org/10.1016/j.jmatprotec.2008.09.034>
4. Aslantas, K.; Ekici, E.; Çiçek, A. Optimization of process parameters for micro milling of Ti-6Al-4V alloy using Taguchi-based gray relational analysis. *Measurement* **2018**, *128*, 419–427. <https://doi.org/10.1016/j.measurement.2018.06.051>
5. Ezugwu, E.O. Key improvements in the machining of difficult-to-cut aerospace superalloys. *Int. J. Mach. Tools Manuf.* **2005**, *45*, 1353–1367. <https://doi.org/10.1016/j.ijmachtools.2005.02.003>
6. Kang, A.S.; Cheema, G.S.; Gandhi, V. Optimization of Surface Roughness and Metal Removal Rate in End Milling using Taguchi Grey Relational Analysis. *Indian J. Sci. Technol.* **2017**, *10*(31), 115447. <https://doi.org/10.17485/ijst/2017/v10i31/115447>
7. Senthilkumar, K.M.; Thirumalai, R.; Selvam, T.A. et al. Multi objective optimization in machining of Inconel 718 using Taguchi method. *Mater. Today Proc.* **2021**, *37*, 3466–3470. <https://doi.org/10.1016/j.matpr.2020.09.281>
8. Titu, A.M.; Sandu, A.V.; Pop, A.B. et al. Design of Experiment in the Milling Process of Aluminum Alloys in the Aerospace Industry. *Materials* **2020**, *13*(19), 4426. <https://doi.org/10.3390/ma13194426>
9. Verma, G.C.; Pandey, P.M. Machining forces in ultrasonic-vibration assisted end milling. *Ultrasonics* **2019**, *94*, 350–363. <https://doi.org/10.1016/j.ultras.2018.05.010>
10. Kumaran, D.; Paramasivam, S.S.S.; Natarajan, H. Optimization of high speed machining cutting parameters for end milling of AlSi7Cu4 using Taguchi based technique of order preference similarity to the ideal solution. *Mater. Today Proc.* **2021**, *47*, 6799–6804. <https://doi.org/10.1016/j.matpr.2021.05.062>
11. Wang, Z.; Li, L. Optimization of process parameters for surface roughness and tool wear in milling TC17 alloy using Taguchi with grey relational analysis. *Adv. Mech. Eng.* **2021**, *13*(2), 1–8. <https://doi.org/10.1177/1687814021997428>
12. Seçgin, O.; Sogut, M.Z. Surface roughness optimization in milling operation for aluminum alloy (Al 6061-T6) in aviation manufacturing elements. *Aircr. Eng. Aerosp. Technol.* **2021**, *93*(9), 1490–1498. <https://doi.org/10.1108/AEAT-03-2021-0076>
13. Mall, V.K.; Kumar, P.; Singh, B. A Review of Optimization of Surface Roughness of Inconel 718 in End Milling using Taguchi Method. *Int. J. Eng. Res. Appl.* **2014**, *4*(12), 103–109.
14. Tsao, C.C. Grey–Taguchi method to optimize the milling parameters of aluminum alloy. *Int. J. Adv. Manuf. Technol.* **2009**, *40*, 41–48. <https://doi.org/10.1007/s00170-007-1304-5>
15. Ghani, J.A.; Choudhury, I.A.; Hassan, H.H. Application of Taguchi method in the optimization of end milling parameters. *J. Mater. Process. Technol.* **2004**, *145*, 84–92. [https://doi.org/10.1016/S0924-0136\(03\)00865-3](https://doi.org/10.1016/S0924-0136(03)00865-3)

**Publisher’s Note:** IIKII stays neutral with regard to jurisdictional claims in published maps and institutional affiliations.



© 2025 The Author(s). Published with license by IIKII, Singapore. This is an Open Access article distributed under the terms of the [Creative Commons Attribution License](https://creativecommons.org/licenses/by/4.0/) (CC BY), which permits unrestricted use, distribution, and reproduction in any medium, provided the original author and source are credited.